

# On six-loop scaling dimensions of $(\phi^2)^n$ operators in $d = 3$

A. V. Bednyakov<sup>1</sup>, M. V. Kompaniets<sup>1,2</sup> and A. V. Trenogin<sup>1,2</sup>

<sup>1</sup>*Bogoliubov Laboratory of Theoretical Physics, Joint Institute for Nuclear Research,  
Dubna 141980, Russian Federation*

<sup>2</sup>*Saint Petersburg State University, 7/9 Universitetskaya nab., St. Petersburg 199034,  
Russian Federation*

## Abstract

We consider a class of singlet operators  $(\phi^2)^n$  in the three-dimensional  $O(N)$  model with  $\lambda^2\phi^6$  interaction. Recently [1], the corresponding anomalous dimensions  $\gamma_{2n}$  were computed by semiclassical methods and the all-loop result for the leading- $n$  corrections in the small  $\lambda$  limit was found. In this letter, we obtain the six-loop expressions not only for the leading- $n$  contribution but also for the subleading one. While the leading correction confirms the predictions of recent semiclassical calculation, the subleading one is a new result and will serve as a future welcome check for the all-loop expressions. As an important by-product of our calculation, we provide a full dependence on  $n$  of the four-loop  $\gamma_{2n}$  in the  $O(N)$  case.

## 1 Introduction

In high-energy physics, quantum field theory (QFT) is the main tool used to describe various phenomena observed at experiment. A major role in QFTs is played by renormalization group (RG) that among other things encodes the scale dependence of the Lagrangian parameters. Renormalizable QFT models, such as the Standard Model (SM), has a finite set of parameters giving rise to a high predictive power across a wide range of energy scales. Nevertheless, it is believed that renormalizable QFTs in  $d$  space-time dimensions are nothing else but (low-energy) effective field theories (EFT), in which we neglect an infinite tower of local composite operators  $\{O_i(x)\}$ . A common approach is to order the latter by their canonical dimensions  $d_{O_i} > d$ . Such operators enter into the Lagrangian with couplings (Wilson coefficients)  $c_i$  of negative mass dimension  $d_{c_i} = d - d_{O_i} < 0$ , and one can easily convince oneself that their contributions are suppressed in the infra-red (IR) region. Nevertheless, one can consistently include corrections due to these operators by truncating the infinite set and keeping only those  $O_i$  that have  $d_{O_i} \leq d_{\max}$  for some fixed  $d_{\max}$  (see, e.g., Refs. [2, 3] and references therein).

For phenomenological applications, it is important to know how the Wilson coefficients  $c_i$  change with renormalization scale  $\mu$ . The corresponding RG functions are directly related to the operator anomalous dimensions (ADs). The latter can be calculated in the perturbation theory (PT) at weak coupling  $\lambda$ .

One can also apply QFT to study second-order phase transitions (see, e.g., a review [4] and a textbook [5]). The anomalous dimensions evaluated at a infra-red fixed point (FP)  $\lambda^*$  become observable quantities corresponding to various critical exponents  $\Delta$ . One can routinely use PT to compute the latter as series in  $\varepsilon$  [6], which is a deviation of physical dimension  $d = d_0 - 2\varepsilon$  from the logarithmic one  $d_0$ , in which the coupling  $\lambda$  is dimensionless.

At criticality, physical systems usually exhibit universal behavior, which can also be described by a conformal field theory (CFT), see, e.g., recent [3] and references therein. Application of the CFT methods to critical phenomena can go beyond the usual PT and allows one to study the strong-coupling regime of the model. Due to this, comparison between perturbative and non-perturbative results plays an important role in understanding QFT models. Establishing the connection between the quantities computed in PT and non-perturbatively works both ways. From one side, non-perturbative results can extend the applicability of expressions computed at a fixed order of PT (e.g., by certain re-summation of PT series). From the other side, such a comparison can provide a convenient (QFT) interpretation of quantities computed within CFTs.

Among recent examples, let us mention a vast literature on the so-called large-charge expansion (see, e.g., Ref. [7, 8, 9]), in which one introduces a 't Hooft-like coupling  $\lambda Q$ , rewrites the scaling dimension of the lowest-lying operator with charge  $Q$  as

$$\Delta_Q = \sum_{j=-1}^{\infty} \frac{\Delta_j(\lambda^* Q)}{Q^j} \quad (1)$$

and derives all-loop results for the leading- $Q$  ( $\Delta_{-1}$ ) and subleading- $Q$  ( $\Delta_0$ ) terms via a semiclassical calculation. It is worth to mention that direct comparison with diagrammatic computations (see, e.g, Ref. [10, 11, 12, 13, 14, 15]) beyond one-loop order demonstrates that the anomalous dimensions obtained by the above-mentioned non-perturbative method precisely match standard PT calculations, even away from the FP.

Recently, the semiclassical method was extended to account for the spinless neutral operators of the form  $(\phi^2)^n$  [1], and a similar expansion (1) for the scaling dimension  $\Delta_{2n}$  was computed in the leading- $n$  [1] approximation for  $d_0 = 3, 4, 6$ . The subleading- $n$  terms for Ising CFT at  $d_0 = 4$  were derived in [16] together with a bunch of new results for the operators with spin. The authors of Ref. [1] compared their leading- $n$  prediction with available lowest-order results and find perfect agreement.

In this letter, we restrict ourselves to  $d_0 = 3$  and consider both leading- $n$  and subleading- $n$  contributions to the anomalous dimensions  $\gamma_{2n}$  of spinless  $(\phi^2)^n$  operators<sup>1</sup> in the  $O(N)$  model with  $\lambda^2\phi^6$  interaction. To do this we use the following Euclidean Lagrangian

$$\mathcal{L} = \frac{Z_1}{2}(\partial_\nu\phi \cdot \partial_\nu\phi) + \frac{Z_3}{6}\lambda^2\mu^{4\varepsilon}(\phi^2)^3, \quad [\phi] = \frac{1}{2} - \varepsilon, \quad (2)$$

where we suppress  $O(N)$  indices of the scalar field  $\phi = \{\phi^a, a = 1, \dots, N\}$  in fundamental representation of the group. The same model with an additional mass term can be applied in statistical physics for systems with tricritical points, as demonstrated in Ref. [5]. These points have been experimentally observed in various systems (see Refs. [5, 17] and the references therein). Such systems show different asymptotic behaviors when approaching the tricritical point, depending on the trajectory taken in the physical parameter space. These behaviors arise naturally from the analysis of the  $\phi^4 + \phi^6$  model<sup>2</sup> [5, 18, 19]. For a trajectory for which the  $\phi^4$  interaction near the tricritical point is more significant than the  $\phi^6$  one, the latter becomes irrelevant, and the corresponding *modified* critical behavior can be studied by means of the  $\phi^4$  model<sup>3</sup>. On the other hand, if the  $\phi^6$  interaction dominates, this behavior becomes tricritical and can be described by the  $\phi^6$  model with corresponding tricritical exponents [20, 21, 22, 23, 24]. Additionally, in Ref. [5] a situation explored when both interactions are equally significant (so-called combined tricriticality[5]). However, this possibility has not been well studied yet and calls for an additional investigation (see Ref. [24]). Let us also mention that the phenomenon is also studied using various simulations in different models, e.g., in the Blum-Capel or Blum-Emery-Griffith models (see Refs. [25, 26, 27]).

The renormalization constants  $Z_1$  and  $Z_3$  entering into (2) are known up to six loops [21, 22, 23, 24] and introduced to render all the Green functions involving the  $\phi$  fields finite. In what follows we routinely use dimensional regularization [28], i.e., we work in  $d = 3 - 2\varepsilon$ , together with (modified) minimal subtraction scheme  $\overline{\text{MS}}$  [29]. In the latter scheme, the renormalization constants are functions of dimensionless coupling  $\lambda$ , which depends on the renormalization scale  $\mu$ .

In perturbation theory (i.e., small  $\lambda$  limit) the anomalous dimension can be represented as<sup>4</sup>

$$\gamma_{2n} = \mathfrak{n} \sum_{l=1}^{\infty} \lambda^{2l} P_{2l}(\mathfrak{n}), \quad P_m(x) = \sum_{k=0}^m C_{m,k}(N) \cdot x^{m-k}, \quad \mathfrak{n} \equiv 2n, \quad (3)$$

<sup>1</sup>Strictly speaking, an eigenoperator with certain scaling dimension, which in the lowest order coincides with  $(\phi^2)^n$ .

<sup>2</sup>It should be noted that the critical and tricritical points also differ in the behavior when a system approaches them. When approaching the critical point, the coupling of the  $\phi^4$  interaction tends to a non-zero constant, while in the vicinity of the tricritical point it tends to zero. As a consequence, various situations become possible when approaching the tricritical point.

<sup>3</sup>The corresponding *modified* critical exponents are not the same as in the usual critical situation, in which the  $\phi^4$  coupling remains non-zero constant at the fixed point. Nevertheless, the modified exponents can be easily recomputed from the critical ones [5].

<sup>4</sup>We use  $\mathfrak{n}$  (the number of fields in the operator) as an argument of the polynomials  $P_{2l}$  for convenience, allowing one to easily compare with Ref. [1].

where the sum over  $l$  corresponds to loop expansion, and  $P_m(x)$  is a degree- $m$  polynomial with coefficients  $C_{m,k}$  depending on  $N$ . One can see that at each order of PT all  $C_{2l,k}$  with  $k = 0, \dots, 2l$  can be determined by considering the anomalous dimensions  $\gamma_{2k}$  for fixed  $k = 1, \dots, 2l+1$ . Due to the  $O(N)$  symmetry<sup>5</sup>, this is not an easy task at high PT orders. For example, at six loops one needs to consider the family of all operators from  $\phi^2$  up to  $(\phi^2)^7$  to reconstruct the full dependence on  $n$ .

The model (2) exhibits a fixed point [21, 22, 23]

$$\frac{\lambda^{*2}}{8\pi^2} = \frac{\varepsilon}{3N+22} + \mathcal{O}(\varepsilon^2) \quad (4)$$

resulting in a Conformal Field Theory (CFT). Substituting (4) into (3), we obtain

$$\gamma_{2n}(\lambda^*) \equiv \gamma_{2n}^* = \mathfrak{n} \sum_{l=1}^{\infty} (2\varepsilon)^l P_{2l}^*(\mathfrak{n}), \quad P_m^*(x) = \sum_{k=0}^m \frac{D_{m,k}(N)}{(3N+22)^{m-1}} \cdot x^{m-k}, \quad \mathfrak{n} \equiv 2n \quad (5)$$

that defines a scaling dimension of the corresponding operator

$$\Delta_{2n} = n(1 - 2\varepsilon) + \gamma_{2n}^* \quad (6)$$

and represents an important ingredient of the CFT data. The all-loop result of Ref. [1] expanded in the weak coupling limit allows one to compute all the leading- $n$  coefficients, i.e., all  $C_{2l,0}$  (and  $D_{2l,0}$ ).

The main aim of the paper is to use diagrammatic approach to obtain the expressions both for leading  $C_{2l,0}$  and for subleading  $C_{2l,1}$  up to six loops. As a consequence, our results not only confirm the findings of Ref. [1], but also provide a useful input and a cross check for subsequent semi-classical studies [30].

The paper is organized as follows. In Section 2, we discuss the renormalization of the  $(\phi^2)^n$  operators together with the subtlety related to its mixing with operators involving  $2(n-2)$  fields. To compute the required contributions, we introduce a set of auxiliary operators together with auxiliary diagrams, which we describe in Sec. 3. Our results for the six-loop leading and subleading- $n$  corrections to  $\gamma_{2n}$  and for the complete dependence on  $n$  of the four-loop  $\gamma_{2n}^{(4)}$  can be found in Sec. 4. We conclude in Sec. 5. In Appendices one can find additional information on operators with  $2(n-2)$  fields (appendix A); our treatment of quadratically divergent diagrams (appendix B.1) and all required counterterms for six-loop diagrams (appendix B.2).

## 2 Renormalization of $(\phi^2)^n$ : leading- $n$ and subleading- $n$ orders

We study the local  $(\phi^2)^n$  operator, which following Ref. [31] can be represented graphically as

$$O_n^{(n)} = (\phi^2)^n \rightarrow \underbrace{\bullet \bullet \dots \bullet \bullet}_n. \quad (7)$$

Here, and in what follows, we use  $O_{m,k}^{(n)}$  to denote  $k$ -th<sup>6</sup> operator with canonical dimension  $n$  (in  $d=3$ ) constructed from  $2m$  fields. The picture shows the structure of the operator by representing each field  $\phi = \{\phi^a, a = 1, \dots, N\}$  by a dot. The fields/dots are arranged into  $n$  columns corresponding to  $O(N)$  contractions  $\phi^a \phi^a = \phi^2$ . The corresponding Feynman rule looks like

$$O_n^{(n)} \rightarrow (2n)!! [\delta^{a_1 a_2} \dots \delta^{a_{2n-1} a_{2n}} + \text{perms}], \quad (8)$$

where  $a_1, \dots, a_{2n}$  are  $O(N)$  indices of the external legs, and there are  $(2n-1)!! = (2n)!/(2n)!!$  terms in the brackets.

To compute the anomalous dimension (matrix), we consider one-particle-irreducible (1PI) Green functions with an operator insertion, which can be written as

$$\Gamma_k^{a_1, \dots, a_k} [O](Q, q_1, \dots, q_k) = \int d^D x e^{-iQx} \left[ \prod_{i=1}^k d^D x_i e^{-iq_i x_i} \right] \langle O(x) \phi^{a_1}(x_1) \dots \phi^{a_k}(x_k) \rangle_{1\text{PI}}. \quad (9)$$

<sup>5</sup>In the case of  $N=1$  we can use half-integer  $n$  as a constraint on  $\gamma_{2n}$ .

<sup>6</sup>We omit  $k$  if there is a single operator for fixed  $n$  and  $m$ .

Here we restrict ourselves only to a singlet composite operator  $O(x)$ , with  $\phi^{a_i}$  being fields (order parameter) in fundamental representation of the  $O(N)$  group. To be as general as possible, we introduce a non-zero momentum  $Q$  flowing into the operator vertex. For brevity, we will use a condensed notation

$$\Gamma_k[O] = \sum_l \Gamma_k^{(2l)}[O]$$

for (9) and its  $2l$ -loop contribution, thus, omitting the external  $O(N)$  indices together with the momentum dependence of the Green functions.

When the operator (7) is inserted into the Green functions (9) with different number  $\phi$ 's, new ultra-violet (UV) divergences are generated, thus, requiring the operator to be renormalized in addition to fields and couplings of the model. A common situation is the mixing between a family of the operators, which results in the following relation between renormalized and bare operators:

$$[O_i]_R = Z_{ij}(O_j)_{\text{bare}}, \quad Z_{ij} = \sum_{l=1}^{\infty} Z_{ij}^{(2l)}, \quad Z_{ij}^{(2l)} = \sum_{k=1}^l \frac{Z_{ij}^{(2l,k)}}{\varepsilon^k}. \quad (10)$$

Here the bare operators are constructed from the bare fields  $\phi_{\text{bare}} = Z_1^{1/2}\phi$ , and the sum over  $l$  corresponds to loop expansion. The anomalous-dimension matrix (in the minimal scheme) can be computed from

$$\gamma_{ij} \equiv -\frac{dZ_{ik}}{d\ln \mu} Z_{kj}^{-1} = \sum_{l=1}^{\infty} \gamma_{ij}^{(2l)}, \quad \gamma_{ij}^{(2l)} = 2(2l) Z_{ij}^{(2l,1)}. \quad (11)$$

In what follows, we routinely use the last equation that relates the  $2l$ -loop contribution  $\gamma_{ij}^{(2l)}$  to the anomalous dimension with the coefficient of the first pole in  $\varepsilon$  of the renormalization constant  $Z_{ij}^{(2l,1)}$ .

A standard approach [5] to calculate anomalous dimensions from (10) and (11) requires one to use a closed system of composite operators  $O_i$  with canonical dimensions equal to (or less than<sup>7</sup>) the dimension of our interest. For example, in  $d = 3$  one can replace four  $\phi$  fields by two derivatives, without affecting the canonical dimension of the operator.

In general, the system of operators can be quite large and a convenient choice can significantly simplify the computations (see, e.g., recent Ref. [3] and references therein). For example, one can set the operator momentum  $Q = 0$  in (9), i.e., instead of “unintegrated” operators we consider the set of “integrated” ones<sup>8</sup>. For the latter case, we do not need to deal with operators that are total derivatives, since they are proportional to  $Q$  in momentum space. Such operators correspond to descendants of primaries in CFT and do not add new information to the CFT data with their anomalous dimensions related to that of primaries.

If we fix  $n$  large enough, we have to consider insertions of  $O_n^{(n)}$  not only into  $2n$ -point functions, which correspond to logarithmically divergent graphs, but also into  $2(n-2)$ ,  $2(n-4)$ , etc. that lead to quadratically and higher divergent diagrams. As a consequence, the number of operators that can appear in the right-hand side (RHS) of (10) proliferate significantly (one can use Hilbert series to count independent operators, see, e.g., [31]). Nevertheless, not all the operators appear as counterterms at lower loops. Due to this, we do not consider general mixing matrix, but use loop-by-loop approach, adding necessary operators, when a new divergent contribution appears.

At two and higher loops, the 1PI  $2n$ -point function with one  $O_n^{(n)}$  insertion is logarithmically divergent. In Fig. 1a we show a two-loop diagram contributing to  $\Gamma_{2n}[O_n^{(n)}]$ . One can see that at the lowest PT order only three (“active” legs) out of  $2n$  legs of the operator enter the 1PI part, while  $2n-3$  (marked by red color) are just “spectators”, i.e., they are directly connected to the external lines  $\phi^{a_i}$ .

Having this in mind, we follow [12] and only consider a class of UV divergent diagrams that gives rise to the leading- $n$  and subleading- $n$  terms in the anomalous dimension  $\gamma_{2n}$ : at  $2l$  loops we select those graphs that have  $2l+1$  and  $2l$  “active” operator legs. We also ignore self-energy insertions into external legs, since they contribute only linearly in  $n$  [12].

<sup>7</sup>e.g., if we consider a massive theory, or allow multiple insertions of certain operators

<sup>8</sup>This precisely corresponds to the procedure, when one introduces (constant) couplings  $c_i$  for a set of operators  $O_i$  and add the terms  $c_i O_i$  to the interaction Lagrangian. The anomalous dimension matrix  $\gamma_{ij}$  of  $O_i$  in this case can be extracted from the linear terms of the  $c_i$  beta functions.

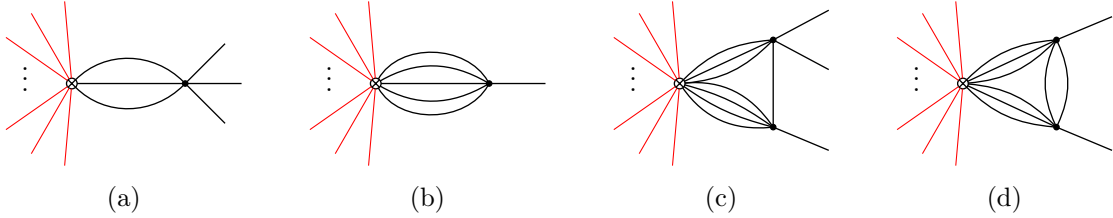


Figure 1: Examples of Feynman diagrams giving rise to divergent contribution to  $\Gamma_{2n}[O_n^{(n)}]$  at two loops (a), and to  $\Gamma_{2n-4}[O_n^{(n)}]$  at four (b) and six (c, d) loops. The “spectator” legs of the operator are marked by the red color. The corresponding auxiliary graphs  $\Gamma_3[\tilde{O}_3^{(n)}]$ ,  $\Gamma_1[\tilde{O}_5^{(n)}]$ ,  $\Gamma_3[\tilde{O}_7^{(n)}]$ , and  $\Gamma_2[\tilde{O}_6^{(n)}]$  for (a), (b) (c), and (d), respectively, are obtained by stripping off the “spectator” lines.

To compute the necessary corrections to  $\gamma_{2n}$ , we apply  $\mathcal{Z}$ -operation to the selected diagrams. The latter associate a local counterterm with a 1PI Green function and in the minimal scheme is given by

$$\mathcal{Z} \equiv -\mathcal{K}\mathcal{R}' \quad (12)$$

with  $\mathcal{R}'$  being incomplete BPHZ  $\mathcal{R}$ -operation, and  $\mathcal{K}$  extracting the pole part from the result. Since  $\mathcal{K}\mathcal{R}'$  of the graphs with cut vertices (vertex-reducible) factorizes and does not produce first poles in  $\varepsilon$ , we safely ignore such diagrams.

There is a number of differences between our computation and that of Ref. [12]. First of all, we have a larger number of logarithmically divergent graphs (see Appendix. B.2), since the fixed-charge operators correspond to traceless symmetric products of  $\phi^a$  so the diagrams leading to contractions between the fixed- $Q$  operator  $O(N)$  indices vanish. Moreover, charged operators do not mix under renormalization with operators involving derivatives.

In our case, at four and higher loops we have a non-zero contribution to the mixing between operators originating from the quadratically divergent graphs  $\Gamma_{2n-4}[O_n^{(n)}]$  (see Fig. 1b-d). As a consequence, we have to consider all possible operators involving two derivatives, which can be written as

$$O_{n-2,1}^{(n)} = (\phi^2)^{n-3}(\phi\partial^2\phi) \quad \rightarrow \quad \begin{array}{c} \bullet \\ \bullet \\ \dots \\ \bullet \\ \bullet \end{array}, \quad (13)$$

$$O_{n-2,2}^{(n)} = (\phi^2)^{n-3}(\partial_\mu\phi\partial_\mu\phi) \quad \rightarrow \quad \begin{array}{c} \bullet \\ \bullet \\ \dots \\ \bullet \\ \bullet \end{array}, \quad (14)$$

$$O_{n-2,3}^{(n)} = (\phi^2)^{n-4}(\phi\partial_\mu\phi)^2 \quad \rightarrow \quad \begin{array}{c} \bullet \\ \bullet \\ \dots \\ \bullet \\ \bullet \\ \bullet \end{array}. \quad (15)$$

Here the lines represent Lorentz contractions of two derivatives  $\partial_\mu$  acting on the corresponding fields. As it was mentioned earlier, we do not include a total-derivative operator  $\partial^2(\phi^2)^{n-2}$  in this list.

Application of  $\mathcal{Z}$  to relevant  $2l$ -loop divergent 1PI Green function with operator insertions can naturally be written as

$$\mathcal{Z}\Gamma_{2n}^{(2l)}[O_n^{(n)}] = \tilde{Z}_{n,n}^{(2l)} \cdot O_n^{(n)} + \mathcal{O}(n^{2l-1}), \quad (16)$$

$$\mathcal{Z}\Gamma_{2(n-2)}^{(2l)}[O_n^{(n)}] = \sum_i \tilde{Z}_{n,n-2,i}^{(2l)} \cdot O_{n-2,i}^{(n)} + \mathcal{O}(n^{2l-1}), \quad (17)$$

where the renormalization constants  $\tilde{Z}_{n,n}^{(2l)}$  and  $\tilde{Z}_{n,n-2,i}^{(2l)}$  contain poles in  $\varepsilon$  and are linear combinations of  $n^{2l+1}$  (leading) and  $n^{2l}$  (subleading) terms.

While the set  $\{O_n^{(n)}, O_{n-2,i}^{(n)}\}$  is directly related to diagram computations, a more convenient basis of operators consists of conformal primaries (“physical” operators) and the so-called EOM-operators, which are redundant due to equation of motions (EOM). The former are annihilated by the generator

of special conformal transformation  $K_\mu$ , while the latter can be dropped from the calculation (see, e.g., [5] and recent [31] for a more elaborate treatment).

To construct the (necessary part) of the physical basis, we notice that  $O_n^{(n)}$  is itself a conformal primary. To find a primary among the  $O_{n-2,i}^{(n)}$  operators, we first use the integration by parts<sup>9</sup>

$$O_{n-2,1}^{(n)} + O_{n-2,2}^{(n)} + 2(n-3)O_{n-2,3}^{(n)} = 0 \quad (18)$$

reducing the number of independent operators from three to two. Then we construct a conformal primary combination  $\bar{O}_{n-2}^{(n)}$  of operators  $O_{n-2,k}^{(n)}$  annihilated by the generator  $K_\mu$ . Following [32], we consider an anzats

$$\bar{O}_{n-2}^{(n)} = aO_{n-2,2}^{(n)} + bO_{n-2,3}^{(n)} \quad (19)$$

and obtain a constraint on the coefficients  $a$  and  $b$  from the requirement (see Appendix A for more detail)

$$K_\mu \bar{O}_{n-2}^{(n)} = 0 \Rightarrow a + b = 0. \quad (20)$$

As a consequence, we confirm [32] that

$$\bar{O}_{n-2}^{(n)} = b(O_{n-2,3}^{(n)} - O_{n-2,2}^{(n)}) = b(\phi^2)^{n-4} [(\phi \partial_\mu \phi)^2 - \phi^2 (\partial_\mu \phi \partial_\mu \phi)], \quad (21)$$

where  $b$  is an arbitrary constant, which as we will see, will be irrelevant for our computations so we set  $b = 1$ . Given (18) and (21), one can express any operator  $O_{n-2,k}^{(n)}$  in terms of the primary  $\bar{O}_{n-2}^{(n)}$  and  $O_{n-2,1}^{(n)}$ :

$$O_{n-2,2}^{(n)} = -\frac{1}{2n-5} [2(n-3)\bar{O}_{n-2}^{(n)} + O_{n-2,1}^{(n)}] = -\bar{O}_{n-2}^{(n)} + \frac{\bar{O}_{n-2}^{(n)} - O_{n-2,1}^{(n)}}{2n} + \mathcal{O}(n^{-2}), \quad (22)$$

$$O_{n-2,3}^{(n)} = \frac{1}{2n-5} [\bar{O}_{n-2}^{(n)} - O_{n-2,1}^{(n)}] = \frac{\bar{O}_{n-2}^{(n)} - O_{n-2,1}^{(n)}}{2n} + \mathcal{O}(n^{-2}), \quad (23)$$

where we neglect subsubleading- $n$  terms. The operator  $O_{n-2,1}^{(n)}$  is redundant due to EOMs (or can be removed by field redefinitions), i.e.,

$$O_{n-2,1}^{(n)} = (\phi^2)^{n-3} (\phi \partial^2 \phi) = (\phi^2)^{n-3} \phi^a \underbrace{[\partial^2 \phi^a - \lambda^2 \phi^a (\phi^2)^2]}_{\text{EOM}} + \lambda^2 (\phi^2)^n \quad (24)$$

giving rise to additional contribution to the anomalous dimension of the  $O_n^{(n)}$  operator. Equivalently, we can define a class of EOM operators  $\mathcal{E}^{(n)}$

$$\mathcal{E}^{(n)} = O_{n-2,1}^{(n)} - \lambda^2 O_n^{(n)} \quad \Rightarrow \quad \mathcal{E}^{(n)}|_{n-2} = O_{n-2,1}^{(n)}, \quad \mathcal{E}^{(n)}|_n = -\lambda^2 O_n^{(n)}, \quad (25)$$

so that the tree-level insertion of  $\mathcal{E}^{(n)}$  into  $n$  point function denoted as  $\mathcal{E}^{(n)}|_n$  is equivalent to the insertion of  $-\lambda^2 O_n^{(n)}$ , while the insertion of  $\mathcal{E}^{(n)}|_{n-2}$  is equivalent to  $O_{n-2,1}^{(n)}$ .

Explicit computations (see below) show that up to six loops in  $\phi^6$  theory, it is sufficient to consider only these operators to obtain the leading and subleading- $n$  corrections to  $\gamma_{2n}$ . Moreover, following the reasoning of Ref. [33, 31] one can convince oneself that we can ignore the mixing with  $\bar{O}_{n-2}^{(n)}$ . At higher loop orders, one needs to take into account operators with higher number of derivatives together with non-trivial mixing with conformal primaries.

Rewriting RHS of (17) in terms of  $O_n^{(n)}$ ,  $\bar{O}_{n-2}^{(n)}$ , and the EOM-operators  $\mathcal{E}^{(n)}$ , we obtain

$$\mathcal{Z}\Gamma_{2n}^{(2l)}[O_n^{(n)}] = Z_{n,n}^{(2l)} \cdot O_n^{(n)} + Z_{n,\mathcal{E}}^{(2l)} \cdot \mathcal{E}^{(n)}|_n + \mathcal{O}(n^{2l-1}), \quad (26)$$

$$\mathcal{Z}\Gamma_{2n-4}^{(2l)}[O_n^{(n)}] = Z_{n,n-2}^{(2l)} \cdot \bar{O}_{n-2}^{(n)} + Z_{n,\mathcal{E}}^{(2l)} \cdot \mathcal{E}^{(n)}|_{n-2} + \mathcal{O}(n^{2l-1}). \quad (27)$$

<sup>9</sup>This can also be checked from the requirement  $\partial^2[(\phi^2)^{n-2}] = 0$  or by considering the corresponding Feynman rules (see Appendix A) and assuming  $Q = q_1 + \dots + q_{2n-4} = 0$ .

By comparing (17) and (27)

$$Z_{n,n-2}^{(2l)} \bar{O}_{n-2}^{(n)} + Z_{n,\mathcal{E}}^{(2l)} \mathcal{E}^{(n)}|_{n-2} = \sum_i \tilde{Z}_{n,n-2,i}^{(2l)} \cdot O_{n-2,i}^{(n)} \quad (28)$$

$$\begin{aligned} &= \tilde{Z}_{n,n-2,1}^{(2l)} \mathcal{E}^{(n)}|_{n-2} \\ &+ \frac{\tilde{Z}_{n,n-2,2}^{(2l)}}{2n-5} \left[ -(2n-6) \bar{O}_{n-2}^{(n)} - \mathcal{E}^{(n)}|_{n-2} \right] \\ &+ \frac{\tilde{Z}_{n,n-2,3}^{(2l)}}{2n-5} \left[ \bar{O}_{n-2}^{(n)} - \mathcal{E}^{(n)}|_{n-2} \right] \\ &= \frac{\bar{O}_{n-2}^{(n)}}{2n-5} \left[ -(2n-6) \tilde{Z}_{n,n-2,2}^{(2l)} + \tilde{Z}_{n,n-2,3}^{(2l)} \right] \\ &+ \frac{\mathcal{E}^{(n)}|_{n-2}}{2n-5} \left[ (2n-5) \tilde{Z}_{n,n-2,1}^{(2l)} - \tilde{Z}_{n,n-2,2}^{(2l)} - \tilde{Z}_{n,n-2,3}^{(2l)} \right] \end{aligned} \quad (29)$$

we find the relations between the renormalization constants in the “physical” ( $Z_{n,k}$ ) and the initial bases ( $\tilde{Z}_{n,k}$ ):

$$\begin{aligned} Z_{n,n-2}^{(2l)} &= \frac{1}{2n-5} \left[ -(2n-6) \tilde{Z}_{n,n-2,2}^{(2l)} + \tilde{Z}_{n,n-2,3}^{(2l)} \right] \\ &= -\tilde{Z}_{n,n-2,2}^{(2l)} + \frac{\tilde{Z}_{n,n-2,2}^{(2l)} + \tilde{Z}_{n,n-2,3}^{(2l)}}{2n} + \mathcal{O}(n^{2l-1}), \end{aligned} \quad (30)$$

$$\begin{aligned} Z_{n,\mathcal{E}}^{(2l)} &= \frac{1}{2n-5} \left[ (2n-5) \tilde{Z}_{n,n-2,1}^{(2l)} - \tilde{Z}_{n,n-2,2}^{(2l)} - \tilde{Z}_{n,n-2,3}^{(2l)} \right] \\ &= \tilde{Z}_{n,n-2,1}^{(2l)} - \frac{\tilde{Z}_{n,n-2,2}^{(2l)} + \tilde{Z}_{n,n-2,3}^{(2l)}}{2n} + \mathcal{O}(n^{2l-1}). \end{aligned} \quad (31)$$

The “physical” renormalization constant  $Z_{n,n}$  of the conformal primary  $O_n^{(n)}$  can be found from

$$Z_{n,n} - \lambda^2 Z_{n,\mathcal{E}} = \tilde{Z}_{n,n}, \quad (32)$$

so the  $2l$ -loop contribution in the leading- $n$  and subleading- $n$  orders is given by

$$Z_{n,n}^{(2l)} = \tilde{Z}_{n,n}^{(2l)} + \lambda^2 \left[ \tilde{Z}_{n,n-2,1}^{(2l)} - \frac{\tilde{Z}_{n,n-2,2}^{(2l)} + \tilde{Z}_{n,n-2,3}^{(2l)}}{2n} \right] + \mathcal{O}(n^{2l-1}). \quad (33)$$

This equation turns out to be sufficient to extract relevant corrections to  $\gamma_{2n}$  up to six loops.

### 3 Computation technique

To account for the fact that we can choose any  $k$  “active” lines (in our two-loop example in Fig. 1a  $k = 3$ ) out of  $2n$  operator legs, we use the following trick. We introduce a set of auxiliary operators  $\tilde{O}_k^{(n)}$  involving dummy fields  $\hat{\phi}$  with  $k$  external lines that have the Feynman rules

$$\tilde{O}_k^{(n)} \rightarrow \frac{1}{(\hat{\phi}^2)^n} \left[ \prod_{i=1}^k \frac{\partial}{\partial \hat{\phi}^{a_i}} \right] \left( \hat{\phi}^2 \right)^n. \quad (34)$$

For example,

$$\tilde{O}_3^{(n)} \rightarrow \frac{(2n-4)(2n-2)(2n)}{(\hat{\phi}^2)^3} \hat{\phi}^a \hat{\phi}^b \hat{\phi}^c + \frac{(2n-2)(2n)}{(\hat{\phi}^2)^2} \left[ \hat{\phi}^a \delta^{bc} + \hat{\phi}^b \delta^{ac} + \hat{\phi}^c \delta^{ab} \right]. \quad (35)$$

Here, the first term gives rise to the leading- $n$  contribution and accounts for the choice, when all three “active” legs with  $O(N)$  indices  $a, b$  and  $c$  belong to different contracted pairs in the  $(\phi^2)^n$  operator<sup>10</sup>.

<sup>10</sup>Equivalently, belong to different Kronecker deltas in the Feynman rule (8), and, when inserted into  $(2n)$ -point 1PI function, are contracted with some of the “spectator” legs (represented by  $\hat{\phi}$ ).

The subsequent terms in (35) contribute at the subleading- $n$  order and correspond to situation when two ‘‘active’’ legs, e.g.,  $b$  and  $c$  entering into  $\delta^{bc}$  belong to a single contracted pair  $\phi^2$  in the initial operator, while the third leg with index  $a$  is contracted with a spectator one. By considering these auxiliary operators, we can ignore the ‘‘spectator’’ legs, e.g., replace the diagram shown in Fig. 1a by an equivalent diagram corresponding to  $\Gamma_3[\tilde{O}_3^{(n)}]$ , which we for brevity denote as 3-3.

Obviously, for two-, four-, and six-loop contributions to  $\gamma_{2n}$  we need to consider the logarithmically divergent diagrams corresponding to 3-3, 5-5 and 4-4, 7-7 and 6-6 auxiliary graphs, respectively [12].

To generate relevant auxiliary diagrams, we use independently the recent version 4.0 of **qgraf** [34] and a python library **GraphState** [35]. We encode the corresponding expressions as products of three factors, which schematically can be represented as

$$[\text{symmetry factor}] \times [O(N) \text{ factor}] \times [\text{loop integral}].$$

Here the  $O(N)$  factor originates from the Feynman rules, and the loop integral is represented by a graph corresponding to the product of propagator denominators. It is worth mentioning that we do not explicitly consider loop integration but use pre-computed tables for the results of  $\mathcal{KR}'$  (see Appendix B.2), which directly associate a counterterm with the corresponding graph given in the Nickel notation<sup>11</sup>.

To deal with  $O(N)$  indices, we use **FORM** [36, 37, 38, 39]. While the initial expression for  $\Gamma_k[\tilde{O}_k^{(n)}]$  is a tensor involving  $k$  open  $O(N)$  indices  $a_1, \dots, a_k$ , we contract the latter with  $\hat{\phi}^{a_1} \dots \hat{\phi}^{a_k} / k!$  to account for permutations of  $k$  external legs and cancel the powers of  $(\hat{\phi}^2)$  appearing in denominators due the Feynman rule (34).

As it was mentioned earlier, we should also account for divergent  $\Gamma_{2n-4}[O_n^{(n)}]$ . For this purpose, we consider a single 5-1 auxiliary graph at four loops (corresponding to Fig. 1b), and the six-loop auxiliary diagrams<sup>12</sup> 7-3 and 6-2 (examples are given in Fig. 1c-d). Obviously, we are *not allowed* to nullify the momentum  $Q$  flowing into the auxiliary operator<sup>13</sup>, because it is related to the total momentum of the spectator legs. We summarize the types of the auxiliary graphs considered in this paper in Table 1.

Contrary to the case of logarithmically divergent diagrams, for which we can use infra-red rearrangement trick [40] to compute  $\mathcal{KR}'$  (i.e., nullify all but 2 external momenta), for quadratically divergent diagrams the corresponding  $\mathcal{KR}'$  operation depends on the external momenta of the graph. As a consequence, we should keep this dependence to account for the mixing with  $O_{n-2,i}^{(n)}$  operators involving  $2(n-2)$  fields (see Appendix B.1 for our treatment of such diagrams). To distinguish contributions associated with operators  $O_{n-2,i}^{(n)}$ , we first contract  $\Gamma_k[\tilde{O}_{k+4}^{(n)}]$  with the product of *different* auxiliary fields  $\hat{\phi}_1^{a_1} \dots \hat{\phi}_k^{a_k} / k!$ , then make an identification

$$(q_i^2) \rightarrow -(\hat{\phi}^2)^2 O_{n-2,1}^{(n)}, \quad (36)$$

$$(q_i q_j)(\hat{\phi}_i \cdot \hat{\phi}_j) \rightarrow -(\hat{\phi}^2)^3 O_{n-2,2}^{(n)}, \quad (37)$$

$$(q_i q_j)(\hat{\phi}_i \cdot \phi)(\hat{\phi}_j \cdot \phi) \rightarrow -(\hat{\phi}^2)^4 O_{n-2,3}^{(n)}, \quad \phi = \{\hat{\phi}, \hat{\phi}_k\}, \quad k \neq i \neq j, \quad (38)$$

and, finally, replace all the remaining  $\hat{\phi}_i$  by  $\hat{\phi}$  to remove completely the dependence on dummy fields  $\hat{\phi}$ . In the above expressions the momentum  $q_i$  and the field  $\hat{\phi}_i$  are associated with the  $i$ -th external non-operator leg.

<sup>11</sup>For example, **e** · · · **e**111|**eee**| and **eee**111|| for  $\Gamma_{2n}^{(2)}[O_n^{(n)}]$  and auxiliary  $\Gamma_3^{(2)}[\tilde{O}_3^{(n)}]$  in Fig. 1a, respectively.

<sup>12</sup>Of course, 5-1 also contribute at six loops, but at the subsubleading order, so we ignore it.

<sup>13</sup>For example, in this case we completely miss the contribution 5-1 in Fig. 1b.

	2 loops	4 loops	6 loops
leading- $n$	3-3	5-5, 5-1	7-7, 7-3
subleading- $n$	3-3	5-5, 5-1, 4-4	7-7, 7-3, 6-6, 6-2

Table 1: Types of auxiliary diagrams needed to compute  $\gamma_{2n}$  at the leading and subleading order in  $n$  in perturbative theory up to six loop. The notation  $k-m$  corresponds to the insertion of the operator  $\tilde{O}_k^{(n)}$  into  $m$ -point 1PI Green function  $\Gamma_m[\tilde{O}_k^{(n)}]$ . In the case of quadratically divergent diagrams (marked by red color), we have to keep the momentum  $Q$  flowing into the auxiliary operator vertex non-zero (e.g., for diagrams in Fig. 1b-d).

## 4 Results

Let us summarize the results of our computations. In the initial operator basis, the coefficients of the first pole in  $\varepsilon$  of  $\tilde{Z}_{n,n}^{(2l)}$  are given by

$$2 \cdot 2 \cdot \tilde{Z}_{n,n}^{(2,1)} = \frac{\lambda^2}{64\pi^2} \left[ \frac{40n^3}{3} + 8[N-1]n^2 - 40n^2 \right] + \mathcal{O}(n), \quad (39)$$

$$2 \cdot 4 \cdot \tilde{Z}_{n,n}^{(4,1)} = -\frac{\lambda^4}{(64\pi^2)^2} \left[ 1400n^5 + 4(380 + 9\pi^2)[N-1]n^4 - 900(12 - \pi^2)n^4 \right] + \mathcal{O}(n^3), \quad (40)$$

$$\begin{aligned} 2 \cdot 6 \cdot \tilde{Z}_{n,n}^{(6,1)} = & \frac{\lambda^6}{(64\pi^2)^3} \left[ \frac{2516800}{9}n^7 + \frac{16}{9}(246460 + 4794\pi^2 + 81\pi^4)[N-1]n^6 \right. \\ & \left. - \frac{400}{9}(72812 - 2490\pi^2 - 405\pi^4)n^6 \right] + \mathcal{O}(n^5), \end{aligned} \quad (41)$$

with 3-3, 4-4 and 5-5, 7-7 and 6-6 contributing at two loops, at four loops, and at six loops, respectively. Necessary contributions to non-diagonal elements  $\tilde{Z}_{n,n-2,i}^{(2l)}$  can be found from the corresponding divergent auxiliary diagrams. The mixing of  $O_n^{(n)}$  into  $O_{n-2,1}^{(n)}$  becomes non-zero at the four-loop level (5-1)

$$2 \cdot 4 \cdot \tilde{Z}_{n,n-2,1}^{(4,1)} = \frac{\lambda^2}{(64\pi^2)^2} \left[ \frac{8n^5}{3} + \frac{n^4}{3}(16[N-1] - 80) \right] + \mathcal{O}(n^3), \quad (42)$$

$$2 \cdot 6 \cdot \tilde{Z}_{n,n-2,1}^{(6,1)} = -\frac{\lambda^4}{(64\pi^2)^3} \left[ \frac{320n^7}{9} + \frac{n^6}{9}(1472[N-1] + 15680) \right] + \mathcal{O}(n^5), \quad (43)$$

with 7-3 and 6-2 contributing at six loops. The mixing of  $O_n^{(n)}$  into  $O_{n-2,2-3}^{(n)}$  starts at six loops<sup>14</sup>

$$2 \cdot 6 \cdot \tilde{Z}_{n,n-2,2}^{(6,1)} = \frac{\lambda^4}{(64\pi^2)^3} \left[ \frac{256n^7}{3} + 256[N-1]n^6 - 2304n^6 \right] + \mathcal{O}(n^5), \quad (44)$$

$$2 \cdot 6 \cdot \tilde{Z}_{n,n-2,3}^{(6,1)} = -\frac{\lambda^4}{(64\pi^2)^3} \left[ 512n^7 + 1280[N-1]n^6 - \frac{27392}{3}n^6 \right] + \mathcal{O}(n^5), \quad (45)$$

and receive contributions from 7-3 and 6-2. Combining these expressions by means of (33), we compute the required terms in the renormalization constant for  $O_n^{(n)}$  for the physical basis:

$$2 \cdot 2 \cdot Z_{n,n}^{(2,1)} = \frac{\lambda^2}{64\pi^2} \left[ \frac{40n^3}{3} + 8[N-1]n^2 - 40n^2 \right] + \mathcal{O}(n), \quad (46)$$

$$2 \cdot 4 \cdot Z_{n,n}^{(4,1)} = -\frac{\lambda^4}{(64\pi^2)^2} \left[ \frac{4192n^5}{3} + \left( \frac{4544}{3} + 36\pi^2 \right)[N-1]n^4 - \left( \frac{32320}{3} - 900\pi^2 \right)n^4 \right] + \mathcal{O}(n^3), \quad (47)$$

$$\begin{aligned} 2 \cdot 6 \cdot Z_{n,n}^{(6,1)} = & \frac{\lambda^6}{(64\pi^2)^3} \left[ \frac{2516480}{9}n^7 + \frac{16}{9}(246368 + 4794\pi^2 + 81\pi^4)[N-1]n^6 \right. \\ & \left. - \frac{80}{9}(364208 - 12450\pi^2 - 2025\pi^4)n^6 \right] + \mathcal{O}(n^5). \end{aligned} \quad (48)$$

<sup>14</sup>Actually, according to (33) we need only leading- $n$  terms in  $\tilde{Z}_{n,n-2,2-3}^{(2l)}$ .

This allows us to find the leading  $C_{2l,0}$  coefficients in (3) for  $l = 1, 2, 3$ :

$$C_{2,0} = \frac{5}{24\pi^2}, \quad C_{4,0} = -\frac{131}{384\pi^4}, \quad C_{6,0} = \frac{4915}{4608\pi^6}, \quad (49)$$

which perfectly match all-order<sup>15</sup> predictions given in Ref. [1]. In addition, we get the new result for the subleading  $C_{2l,1}$  up to six loops:

$$C_{2,1} = \frac{[N-1]-5}{8\pi^2}, \quad (50)$$

$$C_{4,1} = -\frac{(1136+27\pi^2)[N-1]}{3072\pi^4} - \frac{5(135\pi^2-1616)}{3072\pi^4}, \quad (51)$$

$$C_{6,1} = \frac{(246368+4794\pi^2+81\pi^4)[N-1]}{147456\pi^6} + \frac{5(-364208+12450\pi^2+2025\pi^4)}{147456\pi^6}. \quad (52)$$

It can be shown [5] that the anomalous dimensions of operators for small values of  $n \leq 6$  are related to the anomalous dimensions of parameters and the beta function of the  $\phi^4 + \phi^6$  theory<sup>16</sup>. Using the computed leading and subleading coefficients together with known four-loop results for  $\gamma_2, \gamma_4$  and  $\gamma_6$

$$\gamma_2^{(2)} + \gamma_2^{(4)} = \left( \frac{(N+7)}{12\pi^4} [N-1] + \frac{5}{4\pi^4} \right) \lambda^4, \quad \gamma_2^{(2)} = 0, \quad (53)$$

$$\begin{aligned} \gamma_4^{(2)} + \gamma_4^{(4)} &= \left( \frac{[N-1]}{\pi^2} + \frac{5}{\pi^2} \right) \lambda^2 \\ &- \left( \frac{(8(85N+991)+3\pi^2(N^2+23N+211))}{384\pi^4} [N-1] + \frac{5(1736+135\pi^2)}{128\pi^4} \right) \lambda^4, \end{aligned} \quad (54)$$

$$\begin{aligned} \gamma_6^{(2)} + \gamma_6^{(4)} &= \left( \frac{3}{\pi^2} [N-1] + \frac{25}{\pi^2} \right) \lambda^2 \\ &- \left( \frac{(24(53N+911)+3\pi^2(N^2+35N+655))}{128\pi^4} [N-1] + \frac{45(2248+225\pi^2)}{128\pi^4} \right) \lambda^4. \end{aligned} \quad (55)$$

allows us to reconstruct full dependence on  $n$  of  $\gamma_{2n}$  (3) up to four loops:

$$C_{2,2} = -\frac{[N-1]}{4\pi^2} + \frac{5}{12\pi^2}, \quad (56)$$

$$C_{4,2} = -\frac{(28(5N-121)+9\pi^2(N+19))}{1536\pi^4} [N-1] - \frac{5(2948-405\pi^2)}{1536\pi^4}, \quad (57)$$

$$C_{4,3} = \frac{(8(117N-2153)-3\pi^2(N^2-13N-725))}{3072\pi^4} [N-1] + \frac{25(1976-297\pi^2)}{3072\pi^4}, \quad (58)$$

$$C_{4,4} = -\frac{(8(13N-361)-\pi^2(N^2-N-461))}{512\pi^4} [N-1] - \frac{4472-675\pi^2}{512\pi^4}. \quad (59)$$

In the fixed point

$$\frac{\lambda^{*2}}{8\pi^2} = \frac{\varepsilon}{3N+22} + \frac{(8(53N+911)+\pi^2(N^2+35N+655)) [N-1] + 15(2248+225\pi^2)}{8(3N+22)^3} \varepsilon^2 + O(\varepsilon^3) \quad (60)$$

we find the coefficients of (5) contributing to  $\Delta_{2n}$  at two loops:

$$D_{2,0} = \frac{5}{6}, \quad D_{2,1} = \frac{1}{2}([N-1]-5), \quad D_{2,2} = -\frac{1}{3}(3[N-1]-5) \quad (61)$$

---

<sup>15</sup>We thank the authors of Ref. [1] for sharing with us their prediction for  $C_{6,0}$ .

<sup>16</sup>relations:  $\gamma_2 = -\gamma_\tau = \gamma_{m2}$ ,  $\gamma_4 = -\gamma_\lambda = \gamma_u$ ,  $\gamma_6 = 4\varepsilon + \partial_u \beta(u) = 2\varepsilon + \partial_{\bar{w}_R} \beta(\bar{w}_R)$ ,  $\varepsilon = 2\varepsilon$ . The first equality in notations of the Ref. [5]; the second – [22, 23], where the necessary four-loop results are presented.

and four loops:

$$D_{4,0} = -\frac{131}{24}(3N + 22), \quad (62)$$

$$D_{4,1} = -\frac{1}{192}(3N + 22)\left((1136 + 27\pi^2)[N - 1] - 5(1616 - 135\pi^2)\right), \quad (63)$$

$$D_{4,2} = -\frac{1}{192}\left(4\left\{6(35N^2 - 767N - 5563) + \pi^2(11N^2 + 268N - 2794)\right\}[N - 1] + 200(1999 - 675\pi^2)\right), \quad (64)$$

$$D_{4,3} = \frac{1}{192}\left(\left\{8(669N^2 - 327N - 36347) - 3\pi^2(N^3 - 75N^2 - 3351N - 7415)\right\}[N - 1] + 25(8936 - 11475\pi^2)\right), \quad (65)$$

$$D_{4,4} = -\frac{1}{192}\left(2\left\{8(435N^2 + 2227N - 8081) - \pi^2(3N^3 - 137N^2 - 7585N - 34121)\right\}[N - 1] - 450(8 + 375\pi^2)\right). \quad (66)$$

The two-loop result is

$$\gamma_{2n}^{*(2)} = \mathbf{n}P_2^*(\mathbf{n})(2\varepsilon) = \frac{\mathbf{n}(\mathbf{n} - 2)(5\mathbf{n} + 3N - 8)}{6(3N + 22)}(2\varepsilon) \quad (67)$$

and agrees with the Ref. [41]. The four-loop expression<sup>17</sup> in a case  $N = 1$  is

$$\begin{aligned} \gamma_{2n}^{*(2)} + \gamma_{2n}^{*(4)} &= \frac{\mathbf{n}(\mathbf{n} - 1)(\mathbf{n} - 2)}{30}(2\varepsilon) \\ &- \mathbf{n}\left(\frac{131\mathbf{n}^4 - 1010\mathbf{n}^3 + 1999\mathbf{n}^2 - 1117\mathbf{n} - 18}{15000} + \frac{9(\mathbf{n} - 5)(\mathbf{n} - 2)(\mathbf{n} - 1)}{1600}\pi^2\right)(2\varepsilon)^2. \end{aligned} \quad (68)$$

and matches the result given in Refs. [42, 25]. At the same time, it can be verified that (68) gives the correct four-loop result for  $\gamma_1^* = \frac{\eta}{2}$  (see Refs. [21, 22]).

Only the  $C_{6,0}$  and  $C_{6,1}$  coefficients contribute to the six-loop leading and subleading terms in (5) thus  $D_{6,0}$  and  $D_{6,1}$  can be found:

$$D_{6,0} = \frac{4915}{72}(3N + 22)^2, \quad (69)$$

$$D_{6,1} = \frac{1}{2304}(3N + 22)^2\left((246368 + 4794\pi^2 + 81\pi^4)[N - 1] - 5(364208 - 12450\pi^2 - 2025\pi^4)\right). \quad (70)$$

## 5 Conclusions

We considered a restricted set of Feynman diagrams contributing to the leading- $n$  and subleading- $n$  corrections to the anomalous dimension  $\gamma_{2n}$  of the  $(\phi^2)^n$  operator in  $d = 3 - 2\varepsilon$  dimensions. To deal with operator insertions at generic  $n$ , we split the  $2n$  operator legs into the ‘‘spectator’’ ones and the ‘‘active’’ ones. The former are directly connected to external lines, while the latter correspond to loop propagators and can give rise to UV divergence. At  $2l$  loops, one can only have at most  $2l + 1$  ‘‘active’’ legs, giving rise to at least  $2n - 2l - 1$  spectators for sufficiently large  $n$ . Leading- $n$  and subleading- $n$  terms in  $2l$  loop anomalous dimensions precisely correspond to diagrams with  $2l + 1$  and  $2l$  active legs, respectively. This fact allows us to introduce a set of auxiliary operators (34), involving only the required number of (active) legs, and account for a combinatorial factor related to spectators in the corresponding Feynman rule.

We took into account non-trivial mixing of the neutral operators, which is absent in the fixed-charge case, and obtained the expressions for the leading  $C_{2l,0}$  and subleading  $C_{2l,1}$  coefficients at four ( $l = 2$ ) and six ( $l = 3$ ) loops. The leading coefficients are in full agreement with the ones derived from the all-loop result in Ref. [1]. The four- and six-loop subleading- $n$  terms is our new finding. In subsequent

---

<sup>17</sup>Full four-loop result for the  $O(N)$  case and the computed  $C_{ij}$  and  $D_{ij}$  can be found in supplementary material.

studies it can be compared to subleading semiclassical corrections to  $\Delta_{2n}$  [30]. The latter can be obtained along the lines of Ref. [16].

In addition, we utilized the four-loop results for  $\gamma_2$ ,  $\gamma_4$  and  $\gamma_6$  that are known from literature (see, Eqs. (55) and Refs. [23, 22]), to find the full dependence on  $n$  of the four-loop anomalous dimension  $\gamma_{2n}$  in the  $O(N)$  model for  $d = 3$ . At fixed point, it constitutes an important addition to the CFT data. We are planning to use the same method for  $O(N)$   $\phi^4$ -model in  $d = 4$  and cross-check the result of Ref. [16] for the subleading- $n$  terms in the four-loop approximation. At this loop order in  $\phi^4$ , one has to take into account the operator with four derivatives, corresponding to the auxiliary diagram 5-1, but considered in  $d = 4$ .

Let us also mention that one can try to extend the technique to account for further terms in the large- $n$  expansion: by considering 3-3 auxiliary diagrams at four loops together with subsubleading terms in 5-5, 5-1, and 4-4, we were able to reproduce the correct expression for  $C_{4,2}$  (57).

Finally, let us close by a speculation that while the fixed-charged operators can find their high-energy physics application in processes with many charged particles, the neutral operators considered here can potentially be related to a multi-particle production of states with zero net charge (see, e.g., Ref. [43] and references therein).

## Acknowledgements

We thank O. Antipin, J. Bersini, L. Bork, S. Fedoruk, N. Lebedev, and A. Pikelner for fruitful discussions. We appreciate the authors of Ref. [30] for sharing with us the preliminary results of their paper, confirming our diagrammatic computation.

## A Feynman rules of $O_{n-2,i}^{(n)}$ operators and the conformal primary

In this appendix, we follow Refs. [31, 32] and derive the expression for the conformal primary  $\bar{O}_{n-2}^{(n)}$ . Given the Feynman rules of  $O_{n-2,i}^{(n)}$  in momentum space

$$O_{n-2,1}^{(n)} \rightarrow -(2(n-3))!! \left( \sum_m q_m^2 \right) \left\{ \prod_{i=1}^{n-2} \delta^{a_{2i-1} a_{2i}} + \text{perms} \right\}, \quad (71)$$

$$O_{n-2,2}^{(n)} \rightarrow -(2(n-3))!! \left\{ \left[ \sum_{i=1}^{n-2} 2(q_{2i-1} \cdot q_{2i}) \right] \prod_{i=1}^{n-2} \delta^{a_{2i-1} a_{2i}} + \text{perms} \right\}, \quad (72)$$

$$O_{n-2,3}^{(n)} \rightarrow -(2(n-4))!! \left\{ \left[ \sum_{m \neq m'} (q_m \cdot q_{m'}) - \sum_{i=1}^{n-2} 2(q_{2i-1} \cdot q_{2i}) \right] \prod_{i=1}^{n-2} \delta^{a_{2i-1} a_{2i}} + \text{perms} \right\}, \quad (73)$$

where  $q_m$  and  $a_m$  for  $m = 1, \dots, 2(n-2)$  correspond to the momentum and the  $O(N)$  index of the  $m$ -th external leg, respectively. There are  $(2(n-2)-1)!! = \frac{(2(n-2))!}{(2(n-2))!!}$  non-trivial permutations of the  $O(N)$  indices.

We use the following representation of  $K_\mu$  (see, e.g., Ref. [32])

$$K_\mu = \sum_{i=1}^k \left[ \frac{\partial}{\partial q_i^\mu} + 2q_i^\nu \frac{\partial}{\partial q_i^\nu} \frac{\partial}{\partial q_i^\mu} - q_\mu^i \frac{\partial}{\partial q_i^\nu} \frac{\partial}{\partial q_\nu^i} \right], \quad (74)$$

and apply it to each operator in the anzats (19). Taking into account that both  $O_{n-2,2}^{(n)}$  and  $O_{n-2,3}^{(n)}$

depend only on  $q_i q_j$ ,  $i \neq j$ , but not on  $q_i^2$ , we need only the first term in  $K_\mu$  ( $d = 3$ ):

$$\begin{aligned} K^\mu O_{n-2,2}^{(n)} &\rightarrow -2 \cdot (2(n-3))!! \sum_{j=1}^{n-2} \left[ \frac{\partial}{\partial (q_{2j-1})_\mu} + \frac{\partial}{\partial (q_{2j})_\mu} \right] \left\{ \left[ \sum_{i=1}^{n-2} (q_{2i-1} \cdot q_{2i}) \right] \prod_{i=1}^{n-2} \delta^{a_{2i-1} a_{2i}} + \text{perms} \right\} \\ &= -2 \cdot (2(n-3))!! \left[ \sum_{m=1}^{2(n-2)} q_m^\mu \right] \prod_{i=1}^{n-2} \delta^{a_{2i-1} a_{2i}} + \text{perms}, \end{aligned} \quad (75)$$

$$\begin{aligned} K^\mu O_{n-2,3}^{(n)} &\rightarrow -2 \cdot (2(n-4))!! \sum_{k=1}^{2(n-2)} \frac{\partial}{\partial (q_k)_\mu} \left[ \frac{1}{2} \sum_{m \neq m'} (q_m \cdot q_{m'}) - \sum_{i=1}^{n-2} (q_{2i-1} \cdot q_{2i}) \right] \prod_{i=1}^{n-2} \delta^{a_{2i-1} a_{2i}} + \text{perms} \\ &= -2 \cdot (2(n-4))!! \sum_{k=1}^{2(n-2)} \left[ \sum_{m \neq k} q_m^\mu - q_k^\mu \right] \prod_{i=1}^{n-2} \delta^{a_{2i-1} a_{2i}} + \text{perms} \\ &= -2 \cdot (2(n-4))!! \sum_{k=1}^{2(n-2)} [2(n-3)q_k^\mu] \prod_{i=1}^{n-2} \delta^{a_{2i-1} a_{2i}} + \text{perms}. \end{aligned} \quad (76)$$

Summing these expressions with arbitrary coefficients  $a$  and  $b$ , we get

$$0 = a K^\mu O_{n-2,2}^{(n)} + b K^\mu O_{n-2,3}^{(n)} = -(a+b) \cdot 2 \cdot (2(n-3))!! \left[ \left( \sum_{m=1}^{2(n-2)} q_m^\mu \right) \prod_{i=1}^{n-2} \delta^{a_{2i-1} a_{2i}} + \text{perms} \right] \quad (77)$$

leading to the constraint  $a = -b$  (20).

## B Counterterms of graphs

We have used G-functions [44] to calculate the required diagrams. All the 6-6 diagrams together with  $\mathbf{e11122|222|e1}$  (6-2) are generated during the six-loop renormalization group analysis in the  $\phi^6$  theory. The analysis was performed in Refs. [22, 23], but these papers do not provide individual counterterms for the diagrams. One can only find the counterterm of the  $\mathbf{e11122|222|e1}$  diagram in Ref. [22]. We use this counterterm in Eq. (81). Such diagrams were calculated in another work [24] (yet to be published). As a part of the present study, we computed the counterterms for the 7-7 and 7-3 diagrams. Two logarithmic divergent diagrams  $\mathbf{eeee12|22223|33|eee|}$  and  $\mathbf{eee112|22233|e3|eee|}$  (7-7) were calculated using the  $\mathcal{K}\mathcal{R}^*$  operation instead of the  $\mathcal{K}\mathcal{R}'$  operation. In what follows, we briefly describe how we calculated non-trivial 7-3 and 6-2 diagrams. It is worth pointing that part of the 7-7 and 6-6 diagrams are considered in Ref. [12]. Our results are completely consistent with the results of the reference (see Table 2, 3 in our work and (A19), (A20)<sup>18</sup> in Ref. [12]).

### B.1 $\mathcal{K}\mathcal{R}'$ for quadratically-divergent graphs

Here we briefly describe the method<sup>19</sup> used to compute the superficial divergences of the quadratically divergent *scalar* integrals corresponding to the graph  $\Gamma_k$  involving  $k$  external momenta  $p_1, \dots, p_k$  with  $p_1 + \dots + p_k = 0$  in the  $\overline{\text{MS}}$  scheme. For such a diagram application of  $\mathcal{K}\mathcal{R}'$  operation is a quadratic polynomial in external (off-shell) momenta with coefficients being poles in  $\varepsilon$ . Due to this, we can write an anzatz for the result as

$$\mathcal{K}\mathcal{R}' \cdot \Gamma_k(p_1, \dots, p_k) = \sum_{i < j} p_i p_j A^{ij}(\varepsilon), \quad (78)$$

since the scalar products  $p_i p_j$  with  $i \neq j$  form a basis of Lorentz invariants<sup>20</sup> (see, e.g., Ref. [31, 32]). This representation allows one to compute  $A^{ij}$  by setting all but two external momenta to zero,  $p_k = 0$

<sup>18</sup>There is a typo in (A19) and (A20) in the published article: in the left parts should be  $(64\pi^2)^3$  instead of  $(64\pi^3)^3$ . The typo has been corrected in the latest arXiv version.

<sup>19</sup>We do not use here a general approach of Ref. [45], which is based on the expansion on external momenta and can deal with arbitrary tensor integrals.

<sup>20</sup>Given the conservation of momenta, the invariants  $p_i^2 = - \sum_{j \neq i} (p_i p_j)$ .

for  $k \neq i \neq j$ , together with  $p_i = -p_j = P$ . With this trick, we obtain a propagator-type diagram  $\Gamma_2^{(ij)}$ , in which the momentum  $P$  flows in into the leg  $i$  and flows out of the leg  $j$ . The superficial UV divergence is given by

$$\mathcal{K}\bar{\mathcal{R}}^* \cdot \Gamma_2^{(ij)}(P) = -P^2 A^{ij}(\varepsilon) \quad (79)$$

with incomplete  $\mathcal{R}^*$  operation [46, 47] instead of  $\mathcal{R}'$  to account for possible IR divergences<sup>21</sup> that can be generated by setting some of the external momenta to zero. As a consequence, by considering all possible flows of a single external momentum, one can find all the coefficient  $A^{ij}$ .

In our problem, we use this approach for non-trivial<sup>22</sup> 7-3 (Fig. 1c) and 6-2 (Fig. 1d) auxiliary diagrams, which are, when the operator leg is taken into account, are 4-point and 3-point Green functions:

$$\begin{aligned} \mathcal{K}\mathcal{R}' \left[ \begin{array}{c} q_1 \\ q_2 \\ q_3 \\ \hline Q \end{array} \right] &= \frac{(Q, q_1 + q_2)}{P^2} \cdot \mathcal{K}\mathcal{R}' \left[ \begin{array}{c} P \\ \hline P \end{array} \right] \\ &+ \frac{(Qq_3)}{P^2} \cdot \mathcal{K}\mathcal{R}' \left[ \begin{array}{c} P \\ \hline P \end{array} \right] - \frac{(q_3, q_1 + q_2)}{P^2} \cdot \mathcal{K}\mathcal{R}' \left[ \begin{array}{c} P \\ \hline P \end{array} \right] \\ &= \frac{1}{(64\pi^2)^3} \left[ \frac{4}{9\varepsilon} (Q, q_1 + q_2) + \left[ \frac{1}{9\varepsilon^2} - \frac{28}{27\varepsilon} \right] (Qq_3) - \left[ \frac{1}{9\varepsilon^2} + \frac{8}{27\varepsilon} \right] (q_3, q_1 + q_2) \right] \\ &= \frac{1}{(64\pi^2)^3} \left[ \frac{4}{9\varepsilon} (q_1 + q_2)^2 + \left[ \frac{1}{9\varepsilon^2} - \frac{28}{27\varepsilon} \right] q_3^2 - \frac{24}{27\varepsilon} (q_3, q_1 + q_2) \right], \end{aligned} \quad (80)$$

$$\begin{aligned} \mathcal{K}\mathcal{R}' \left[ \begin{array}{c} q_1 \\ q_2 \\ \hline Q \end{array} \right] &= \frac{(Q, q_1 + q_2)}{P^2} \cdot \mathcal{K}\mathcal{R}' \left[ \begin{array}{c} P \\ \hline P \end{array} \right] - \frac{q_1 q_2}{P^2} \cdot \mathcal{K}\mathcal{R}' \left[ \begin{array}{c} P \\ \hline P \end{array} \right] \\ &= \frac{1}{(64\pi^2)^3} \left[ \left( \frac{1}{9\varepsilon^2} - \frac{28}{27\varepsilon} \right) Q^2 - \left( \frac{2}{9\varepsilon^2} - \frac{8}{27\varepsilon} \right) (q_1 q_2) \right] \\ &= \frac{1}{(64\pi^2)^3} \left[ \frac{q_1^2 + q_2^2}{9\varepsilon^2} - \frac{4[7(q_1^2 + q_2^2) + 12q_1 q_2]}{27\varepsilon} \right]. \end{aligned} \quad (81)$$

<sup>21</sup>In our problem, we do not encounter IR divergences in this procedure.

<sup>22</sup>That are not propagator-type, in which all external  $\phi$  legs are connected to a single vertex.

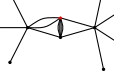
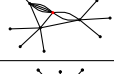
Nickel index	Diagram	$(64\pi^2)^3 \cdot \mathcal{K}\mathcal{R}'$
eeee12 eee33 33333		$\frac{2}{9\epsilon^2} - \frac{40}{27\epsilon}$
eeee12 eee23 33333		$\frac{4}{9\epsilon}$
eeee12 22223 33 eee		$\frac{2}{3\epsilon^2} - \frac{4}{3\epsilon}$
eeee12 ee333 e3333		$\frac{1}{3\epsilon^2}$
eeee12 ee223 3333 e		$\frac{4}{3\epsilon}$
eeee12 e2223 333 ee		$\frac{1}{3\epsilon^2} - \frac{4}{\epsilon}$
eee112 23333 eee3 e		$\frac{2}{3\epsilon^2} - \frac{16}{3\epsilon}$
eee123 ee222 333 ee		$\frac{1}{3\epsilon^3} - \frac{4}{3\epsilon^2} - \frac{8}{3\epsilon}$
eee112 22333 ee3 ee		$\frac{1}{6\epsilon^3} - \frac{2}{\epsilon^2} + \frac{32}{3\epsilon}$
eee112 22233 e3 eee		$\frac{1}{3\epsilon^3} - \frac{8}{3\epsilon^2} + \frac{8}{3\epsilon}$

Table 2: Six-loop logarithmically divergent diagrams in Nickel notation contributing to 7-7 auxiliary graph and their  $\mathcal{K}\mathcal{R}'$ . We highlight the operator insertion by a red pentagon. Only last three diagrams (c.f., Fig. 2a-c of Ref. [12]) contribute to the anomalous dimension of the large-charge operators, which are represented by traceless symmetric products of  $\phi^a$  fields. In the other graphs, the charged operator lines should inevitably hit a Kronecker delta and, thus, the corresponding contribution vanishes.

## B.2 Tables of $\mathcal{K}\mathcal{R}'$

In this appendix, we collect all the relevant six-loop diagrams together with the corresponding results of  $\mathcal{K}\mathcal{R}'$  operation (Tables 2-5). We specify the graph by using either simple Nickel index (for **n-n** diagrams in Tables 2 and 3) or its extension with colored edges [35] (for quadratically divergent integrals 7-3 and 6-2 in Tables 4 and 5, respectively). In the latter case, we use positive integers  $i = 1, 2, 3$  to denote external edges with (outgoing) momentum  $q_i$ , the label -1 specifies the operator insertion (also marked by a red pentagon). The lines marked by 0 correspond to internal propagators.

Nickel index	Diagram	$(64\pi^2)^3 \cdot \mathcal{K}\mathcal{R}'$
eeee12 ee233 3333		0
eeee12 ee233 3333		0
eeee12 22233 33 ee		$-\frac{2\pi^2}{3\varepsilon}$
eeee12 e2333 e333		$\frac{2}{3\varepsilon^2} - \frac{8}{3\varepsilon}$
eeee12 e2233 333 e		$\frac{1}{3\varepsilon^2} - \frac{4}{\varepsilon}$
eee112 eee3 3333		$\frac{2}{9\varepsilon^2} - \frac{40}{27\varepsilon}$
eee112 3333 eee33		$-\frac{2\pi^2}{3\varepsilon}$
eee123 eee23 3333		$\frac{4}{3\varepsilon^2} - \frac{16}{3\varepsilon}$
eee112 ee33 e3333		$-\frac{2\pi^2}{3\varepsilon}$
eee112 ee23 3333 e		$\frac{2}{3\varepsilon^2} - \frac{16}{3\varepsilon}$
ee1112 233 ee33 ee		$\frac{\pi^2(5-2\log 2)}{3\varepsilon} - \frac{\pi^2}{6\varepsilon^2}$
eee123 ee223 333 e		$\frac{1}{6\varepsilon^3} - \frac{2}{\varepsilon^2} - \frac{8(\pi^2-12)}{9\varepsilon}$
eee112 2333 ee33 e		$\frac{1}{6\varepsilon^3} - \frac{2}{\varepsilon^2} - \frac{4(\pi^2-24)}{9\varepsilon}$
eee112 e223 333 ee		$\frac{1}{6\varepsilon^3} - \frac{2}{\varepsilon^2} + \frac{32}{3\varepsilon}$
eee112 2223 33 eee		$\frac{1}{3\varepsilon^3} - \frac{8}{3\varepsilon^2} + \frac{8}{3\varepsilon}$
eee112 2233 e33 ee		$\frac{\pi^2(2\log 2+3)}{3\varepsilon} - \frac{\pi^2}{3\varepsilon^2}$
ee1123 2233 ee3 ee		$\frac{\pi^4}{3\varepsilon}$
eee112 e333 ee333		$\frac{1}{3\varepsilon^3} - \frac{4}{3\varepsilon^2} + \frac{4(\pi^2-6)}{9\varepsilon}$

Table 3: Six-loop logarithmically divergent diagrams in Nickel notation contributing to 6-6 auxiliary graphs and their  $\mathcal{K}\mathcal{R}'$ . We highlight the operator insertion by a red pentagon. Only last eight diagrams contribute to the anomalous dimension of the fixed-charge operators (c.f., Fig. 3a-h of Ref. [12]).

Nickel notation	Diagram	$(64\pi^2)^3 \cdot \mathcal{K}\mathcal{R}'$
<code>eee112 e22222  :1_2_3_0_0_0 -1_0_0_0_0_0  </code>		$\frac{4(q_1+q_2+q_3)^2}{27\epsilon}$
<code>ee1112 e2222 e :1_2_0_0_0_0 -1_0_0_0_0_0 3 </code>		$\frac{q_3^2}{9\epsilon^2} + \frac{4[3(q_1+q_2)^2-7q_3^2-6(q_1+q_2)q_3]}{27\epsilon}$

Table 4: Six-loop quadratically divergent diagrams in Nickel notation contributing to 7-3 auxiliary graphs and their  $\mathcal{K}\mathcal{R}'$ . We keep the operator leg in both the index and the diagram, and use notations of Ref. [35] to denote external momenta  $q_i$ . The first section (before :) is a Nickel index; the second section (after :) labels momenta on external lines. Internal lines we denote as 0, the external leg of the operator as  $-1$  and an external leg with  $q_i$  momentum as  $i$ .

Nickel notation	Diagram	$(64\pi^2)^3 \cdot \mathcal{K}\mathcal{R}'$
<code>ee1122 e2222  :1_2_0_0_0_0 -1_0_0_0_0_0  </code>		0
<code>e11122 e222 e :1_0_0_0_0_0 -1_0_0_0_0 2 </code>		$\frac{q_1^2+q_2^2}{9\epsilon^2} - \frac{4(7q_1^2+12q_2q_1+7q_2^2)}{27\epsilon}$

Table 5: Six-loop quadratically divergent diagrams in Nickel notation contributing to 6-2 auxiliary graphs and their  $\mathcal{K}\mathcal{R}'$ . We keep the operator leg in both the index and the diagram, and use notations of Ref. [35] to denote external momenta  $q_i$ . The first section (before :) is a Nickel index; the second section (after :) labels momenta on external lines. Internal lines we denote as 0, the external leg of the operator as  $-1$  and an external leg with  $q_i$  momentum as  $i$ .

## References

- [1] Oleg Antipin, Jahmall Bersini, and Francesco Sannino. “Exact results for scaling dimensions of neutral operators in scalar conformal field theories”. In: *Phys. Rev. D* 111.4 (2025), p. L041701. DOI: 10.1103/PhysRevD.111.L041701. arXiv: 2408.01414 [hep-th].
- [2] Gino Isidori, Felix Wilsch, and Daniel Wyler. “The standard model effective field theory at work”. In: *Rev. Mod. Phys.* 96.1 (2024), p. 015006. DOI: 10.1103/RevModPhys.96.015006. arXiv: 2303.16922 [hep-ph].
- [3] Johan Henriksson, Stefanos R. Kousvos, and Jasper Roosmale Nepveu. “EFT meets CFT: Multiloop renormalization of higher-dimensional operators in general  $\phi^4$  theories”. In: (Nov. 2025). arXiv: 2511.16740 [hep-th].
- [4] Andrea Pelissetto and Ettore Vicari. “Critical phenomena and renormalization group theory”. In: *Phys. Rept.* 368 (2002), pp. 549–727. DOI: 10.1016/S0370-1573(02)00219-3. arXiv: cond-mat/0012164.
- [5] A. N. Vasil’ev. *The Field Theoretic Renormalization Group in Critical Behavior Theory and Stochastic Dynamics*. Originally published in Russia in 1998 by St. Petersburg Institute of Nuclear Physics Press; translated by Patricia A. de Forcrand-Millard. (see 1.14, 1.16, 4.20–4.23). Chapman and Hall/CRC, London, 2004.
- [6] Kenneth G. Wilson and Michael E. Fisher. “Critical exponents in 3.99 dimensions”. In: *Phys. Rev. Lett.* 28 (1972), pp. 240–243. DOI: 10.1103/PhysRevLett.28.240.

[7] Luis Alvarez-Gaume et al. “Compensating strong coupling with large charge”. In: *JHEP* 04 (2017), p. 059. DOI: 10.1007/JHEP04(2017)059. arXiv: 1610.04495 [hep-th].

[8] Luis Álvarez Gaumé, Domenico Orlando, and Susanne Reffert. “Selected topics in the large quantum number expansion”. In: *Phys. Rept.* 933 (2021), pp. 1–66. DOI: 10.1016/j.physrep.2021.08.001. arXiv: 2008.03308 [hep-th].

[9] Oleg Antipin et al. “Charging the  $O(N)$  model”. In: *Phys. Rev. D* 102.4 (2020), p. 045011. DOI: 10.1103/PhysRevD.102.045011. arXiv: 2003.13121 [hep-th].

[10] Gil Badel et al. “Feynman diagrams and the large charge expansion in  $3-\varepsilon$  dimensions”. In: *Phys. Lett. B* 802 (2020), p. 135202. DOI: 10.1016/j.physletb.2020.135202. arXiv: 1911.08505 [hep-th].

[11] Gil Badel et al. “The Epsilon Expansion Meets Semiclassics”. In: *JHEP* 11 (2019), p. 110. DOI: 10.1007/JHEP11(2019)110. arXiv: 1909.01269 [hep-th].

[12] I. Jack and D. R. T. Jones. “Anomalous dimensions for  $\phi^n$  in scale invariant  $d = 3$  theory”. In: *Phys. Rev. D* 102.8 (2020), p. 085012. DOI: 10.1103/PhysRevD.102.085012. arXiv: 2007.07190 [hep-th].

[13] Qingjun Jin and Yi Li. “Five-loop anomalous dimensions of  $\phi^Q$  operators in a scalar theory with  $O(N)$  symmetry”. In: *JHEP* 10 (2022), p. 084. DOI: 10.1007/JHEP10(2022)084. arXiv: 2205.02535 [hep-th].

[14] Alexander Bednyakov and Andrey Pikelner. “Six-loop anomalous dimension of the  $\phi^Q$  operator in the  $O(N)$  symmetric model”. In: *Phys. Rev. D* 106.7 (2022), p. 076015. DOI: 10.1103/PhysRevD.106.076015. arXiv: 2208.04612 [hep-th].

[15] Rijun Huang, Qingjun Jin, and Yi Li. “From operator product expansion to anomalous dimensions”. In: *JHEP* 06 (2025), p. 135. DOI: 10.1007/JHEP06(2025)135. arXiv: 2410.03283 [hep-th].

[16] Oleg Antipin et al. “Exact Results for the Spectrum of the Ising Conformal Field Theory”. In: (Nov. 2025). arXiv: 2511.08276 [hep-th].

[17] C. Domb and J. L. Lebowitz, eds. *PHASE TRANSITIONS AND CRITICAL PHENOMENA. VOL. 9.* (1. Theory of Tricritical Points, Authors: I. D. Lawrie and S. Sarbach). 1985.

[18] Eberhard K. Riedel. “Scaling Approach to Tricritical Phase Transitions”. In: *Phys. Rev. Lett.* 28 (11 Mar. 1972), pp. 675–678. DOI: 10.1103/PhysRevLett.28.675.

[19] Eberhard K. Riedel and Franz J. Wegner. “Tricritical Exponents and Scaling Fields”. In: *Phys. Rev. Lett.* 29 (6 Aug. 1972), pp. 349–352. DOI: 10.1103/PhysRevLett.29.349.

[20] M.J. Stephen and J.L. McCauley. “Feynman graph expansion for tricritical exponents”. In: *Physics Letters A* 44.2 (1973), pp. 89–90. DOI: 10.1016/0375-9601(73)90799-8.

[21] A. L. Lewis and F. W. Adams. “Tricritical behavior in two dimensions. II. Universal quantities from the  $\epsilon$  expansion”. In: *Phys. Rev. B* 18 (9 Nov. 1978), pp. 5099–5111. DOI: 10.1103/PhysRevB.18.5099.

[22] Johannes Hager and Lothar Schäfer. “ $\Theta$ -point behavior of diluted polymer solutions: Can one observe the universal logarithmic corrections predicted by field theory?” In: *Phys. Rev. E* 60 (2 1999), pp. 2071–2085. DOI: 10.1103/PhysRevE.60.2071.

[23] J. S. Hager. “Six-loop renormalization group functions of  $O(n)$ -symmetric  $\phi^6$ -theory and epsilon-expansions of tricritical exponents up to  $\epsilon^3$ ”. In: *J. Phys. A* 35 (2002), pp. 2703–2711. DOI: 10.1088/0305-4470/35/12/301.

[24] L.Ts. Adzhemyan, M.V. Kompaniets, and A.V. Trenogin. “Renormalization group analysis of tricritical behavior of the  $O(n)$ -symmetric  $\varphi^4 + \varphi^6$  theory up to six loops (in preparation)”. In: () .

[25] Johan Henriksson. “The tricritical Ising CFT and conformal bootstrap”. In: *JHEP* 08 (2025), p. 031. DOI: 10.1007/JHEP08(2025)031. arXiv: 2501.18711 [hep-th].

[26] Leïla Moueddene et al. “Critical and tricritical singularities from small-scale Monte Carlo simulations: the Blume–Capel model in two dimensions”. In: *Journal of Statistical Mechanics: Theory and Experiment* 2024.2 (Feb. 2024), p. 023206. DOI: 10.1088/1742-5468/ad1d60. arXiv: 2401.02720 [cond-mat.stat-mech].

[27] Leïla Moueddene, Nikolaos G. Fytas, and Bertrand Berche. “Critical and tricritical behavior of the  $d = 3$  Blume-Capel model: Results from small-scale Monte Carlo simulations”. In: *Phys. Rev. E* 110.6 (2024), p. 064144. DOI: 10.1103/PhysRevE.110.064144. arXiv: 2410.01710 [cond-mat.stat-mech].

[28] Gerard ’t Hooft and M. J. G. Veltman. “Regularization and Renormalization of Gauge Fields”. In: *Nucl. Phys. B* 44 (1972), pp. 189–213. DOI: 10.1016/0550-3213(72)90279-9.

[29] William A. Bardeen et al. “Deep Inelastic Scattering Beyond the Leading Order in Asymptotically Free Gauge Theories”. In: *Phys. Rev. D* 18 (1978), p. 3998. DOI: 10.1103/PhysRevD.18.3998.

[30] O. Antipin et al. “Semiclassical Canovaccio for Composite Operator (to appear)”. In: (2025).

[31] Weiguang Cao et al. “Renormalization and non-renormalization of scalar EFTs at higher orders”. In: *JHEP* 09 (2021), p. 014. DOI: 10.1007/JHEP09(2021)014. arXiv: 2105.12742 [hep-ph].

[32] Jasper Roosmale Nepveu. “Renormalization and the Double Copy of Effective Field Theories”. PhD thesis. Humboldt-Universität zu Berlin, Humboldt U., Berlin, 2024. DOI: 10.18452/29107.

[33] Zvi Bern, Julio Parra-Martinez, and Eric Sawyer. “Nonrenormalization and Operator Mixing via On-Shell Methods”. In: *Phys. Rev. Lett.* 124.5 (2020), p. 051601. DOI: 10.1103/PhysRevLett.124.051601. arXiv: 1910.05831 [hep-ph].

[34] Paulo Nogueira. “Automatic Feynman Graph Generation”. In: *J. Comput. Phys.* 105 (1993), pp. 279–289. DOI: 10.1006/jcph.1993.1074.

[35] D. Batkovich et al. “GraphState – a tool for graph identification and labelling”. In: (Sept. 2014). arXiv: 1409.8227 [hep-ph].

[36] J. A. M. Vermaasen. “New features of FORM”. In: (Oct. 2000). arXiv: math-ph/0010025.

[37] M. Tentyukov and J. A. M. Vermaasen. “The Multithreaded version of FORM”. In: *Comput. Phys. Commun.* 181 (2010), pp. 1419–1427. DOI: 10.1016/j.cpc.2010.04.009. arXiv: hep-ph/0702279.

[38] J. Kuipers et al. “FORM version 4.0”. In: *Comput. Phys. Commun.* 184 (2013), pp. 1453–1467. DOI: 10.1016/j.cpc.2012.12.028. arXiv: 1203.6543 [cs.SC].

[39] Ben Ruijl, Takahiro Ueda, and Jos Vermaasen. “FORM version 4.2”. In: (July 2017). arXiv: 1707.06453 [hep-ph].

[40] A. A. Vladimirov. “Method for Computing Renormalization Group Functions in Dimensional Renormalization Scheme”. In: *Theor. Math. Phys.* 43 (1980), p. 417. DOI: 10.1007/BF01018394.

[41] Pallab Basu and Chethan Krishnan. “ $\epsilon$ -expansions near three dimensions from conformal field theory”. In: *JHEP* 11 (2015), p. 040. DOI: 10.1007/JHEP11(2015)040. arXiv: 1506.06616 [hep-th].

[42] J. O’Dwyer and H. Osborn. “Epsilon expansion for multicritical fixed points and exact renormalisation group equations”. In: *Annals of Physics* 323.8 (Aug. 2008), pp. 1859–1898. DOI: 10.1016/j.aop.2007.10.005.

[43] S. V. Demidov and B. R. Farkhtdinov. “Numerical study of multiparticle scattering in  $\lambda\phi^4$  theory”. In: *JHEP* 11 (2018), p. 068. DOI: 10.1007/JHEP11(2018)068. arXiv: 1806.10996 [hep-ph].

[44] K.G. Chetyrkin, A.L. Kataev, and F.V. Tkachov. “New approach to evaluation of multiloop Feynman integrals: The Gegenbauer polynomial  $x$ -space technique”. In: *Nuclear Physics B* 174.2 (1980), pp. 345–377. DOI: [https://doi.org/10.1016/0550-3213\(80\)90289-8](https://doi.org/10.1016/0550-3213(80)90289-8).

[45] Franz Herzog and Ben Ruijl. “The  $R^*$ -operation for Feynman graphs with generic numerators”. In: *JHEP* 05 (2017), p. 037. DOI: 10.1007/JHEP05(2017)037. arXiv: 1703.03776 [hep-th].

[46] K. G. Chetyrkin and F. V. Tkachov. “INFRARED R OPERATION AND ULTRAVIOLET COUNTERTERMS IN THE MS SCHEME”. In: *Phys. Lett. B* 114 (1982), pp. 340–344. DOI: 10.1016/0370-2693(82)90358-6.

[47] K. G. Chetyrkin and Vladimir A. Smirnov. “R\* OPERATION CORRECTED”. In: *Phys. Lett. B* 144 (1984). Ed. by A. N. Tavkhelidze et al., pp. 419–424. DOI: 10.1016/0370-2693(84)91291-7.